

A dynamical model for radiatively inefficient accretion flows with convection

Kazem Faghei

School of Physics, Damghan University, Damghan, Iran; *kfaghei@du.ac.ir*

Received 2012 October 11; accepted 2013 May 7

Abstract We explore the time evolution of radiatively-inefficient accretion flows. Since these types of accretion flows are convectively unstable, we also study the effects of convection in the present model. The effects of convection are applied to equations describing angular momentum and energy. In analogy to the traditional α -prescription, we introduce the convection parameter α_c to study the influences of convection on physical quantities. The model is studied in two cases: the transport of angular momentum due to convection inward and outward. We found the physical variables are sensitive to the parameter α_c and are also dependent on the direction of angular momentum that is transported by convection. As for angular momentum transfer inward, the accretion flow can be convectively dominated and radial infall velocity becomes zero. Moreover, we found the radial dependence of the density and radial velocity takes an intermediate place between steady state radiatively-inefficient accretion flow and steady state advection-dominated accretion flow. This property is in accord with direct numerical simulation of radiatively-inefficient accretion flows.

Key words: accretion, accretion disks — convection — hydrodynamics

1 INTRODUCTION

From the current knowledge about accretion disk theory, three types of accretion disk models have been proposed. The criterion is specified by the mass accretion rate onto the central object

$$\dot{M}_{\text{crit}} = \eta \dot{M}_{\text{E}} = \frac{L_{\text{E}}}{c^2},$$

where \dot{M}_{crit} is the critical accretion rate, $\dot{M}_{\text{E}} [= L_{\text{E}}/\eta c^2]$ is the Eddington accretion rate, L_{E} is the Eddington luminosity and η is the efficiency. In the standard theory (Shakura & Sunyaev 1973), the mass accretion rate is subcritical ($\dot{M} \leq \dot{M}_{\text{E}}$). For a very low accretion rate ($\dot{M} \ll \dot{M}_{\text{E}}$), the disk will be assumed to be in the range of an optically-thin advection-dominated accretion flow (optically-thin ADAF) or a radiatively-inefficient accretion flow (RIAFs; Ichimaru 1977; Narayan & Yi 1994; Abramowicz et al. 1995; Popham & Gammie 1998; see also chap. 9 of Kato et al. 2008 for a review). Finally, for a supercritical accretion rate ($\dot{M} \gg \dot{M}_{\text{E}}$), the disk is classified as an optically-thick ADAF or slim disk or supercritical disk (Abramowicz et al. 1988; Mineshige et al. 2000; Fukue 2000, 2009; Watarai & Mineshige 2003).

The observations confirm the existence of RIAFs in the low-luminosity state of X-ray binaries and nuclei of galaxies (Narayan et al. 1996; Esin et al. 1997; Di Matteo et al. 2003; Yuan et al.

2003, 2006; Nemmen et al. 2006; Ho 2009). RIAFs have been considered through direct numerical simulations (e.g. Hawley et al. 2001; Machida et al. 2001; Igumenshchev et al. 2000, 2003; Pen et al. 2003; Igumenshchev 2006; Yuan & Bu 2010) and analytical or semi-analytical methods (Narayan et al. 2000, 2002; Quataert & Gruzinov 2000; Balbus 2004; Lu et al. 2004; Zhang & Dai 2008; Faghei & Omidvand 2012). The direct numerical simulations of low-viscosity RIAFs have confirmed the existence of convective instability in these flows (Igumenshchev et al. 1996, 2000; Igumenshchev & Abramowicz 1999, 2000; Stone et al. 1999; McKinney & Gammie 2002). Thus, the effects of convection have also been considered in RIAF models. Convection simultaneously transports energy outward and angular momentum inward, strongly suppressing the accretion rate onto the central black hole (Narayan et al. 2002).

Analytical or semi-analytical studies of RIAFs have typically been applied to steady state solutions (e.g. Narayan et al. 2000; Lu et al. 2004) and dynamical studies of such systems have been performed by hydrodynamical and magnetohydrodynamical simulations (e.g. Igumenshchev et al. 1996, 2000, 2003; Pen et al. 2003; Yuan & Bu 2010). Ogilvie (1999) presented a model for the time dependence of accretion flow which can be useful for ADAFs and RIAFs. However, Ogilvie did not consider the effects of convection in his model. In this paper, we want to investigate the dynamical behavior of RIAFs in the presence of convection. Thus, we will exploit the model presented by Narayan et al. (2000) to add the influences of convection to the basic equations of Ogilvie's model. The paper is organized as follows. In Section 2, the basic equations of constructing a model for RIAFs in the presence of convection will be defined. In Section 3, an unsteady self-similar method for solving equations, which governs the behavior of the accreting gas, will be used. Results of the model are also presented in Section 3. A summary of the model will be given in Section 4.

2 BASIC EQUATIONS

We adopt the solutions by Ogilvie (1999) and update his model by incorporating the effects of convection in the equations of in angular momentum and energy. Thus, for the dynamical evolution of spherically symmetric accreting and rotating flows under a Newtonian potential from the central object and thermal pressure, we use the compressible Navier-Stokes equations in spherical coordinates (r, θ, φ) . Under these assumptions, the continuity equation is

$$\frac{\partial \rho}{\partial t} + \frac{1}{r^2} \frac{\partial}{\partial r} (r^2 \rho v_r) = 0, \quad (1)$$

where ρ and v_r are the density and accretion velocity ($v_r < 0$), respectively.

The radial momentum equation is

$$\frac{\partial v_r}{\partial t} + v_r \frac{\partial v_r}{\partial r} = r(\Omega^2 - \Omega_K^2) - \frac{1}{\rho} \frac{\partial p}{\partial r}, \quad (2)$$

where Ω is the angular velocity, Ω_K is the Keplerian angular velocity and p is the gas pressure.

The angular momentum equation can be written in the form of a balance between terms representing advection and diffusion transport (Narayan et al. 2000),

$$\rho \left[\frac{\partial}{\partial t} (r^2 \Omega) + v_r \frac{\partial}{\partial r} (r^2 \Omega) \right] = \frac{1}{r^2} \frac{\partial}{\partial r} \left[\nu \rho r^4 \frac{\partial \Omega}{\partial r} \right] + \frac{1}{r^2} \frac{\partial}{\partial r} \left[\nu_c \rho r^{(5+3g)/2} \frac{\partial}{\partial r} \left(\Omega r^{3(1-g)/2} \right) \right], \quad (3)$$

where the two terms on the right-hand side represent the angular momentum transport by viscosity and convection respectively. Here, $\nu [= \alpha p / \rho \Omega_K]$ is the kinematic viscosity coefficient (Shakura & Sunyaev 1973), with α being a constant less than unity, ν_c is the convective diffusion coefficient and g is a parameter that determines the condition of convective angular momentum transport. Generally, convection can transport angular momentum inward (or outward) for $g < 0$ (or > 0), and the specific

case $g = 0$ corresponds to zero angular momentum transport (Narayan et al. 2000). In this paper, we will study two special cases of $g = 1$ and $g = -1/3$ which respectively correspond to

$$\dot{J}_c = -\nu_c \rho r^4 \frac{\partial \Omega}{\partial r} \quad (4)$$

and

$$\dot{J}_c = -\nu_c \rho r^2 \frac{\partial (\Omega r^2)}{\partial r}, \quad (5)$$

where \dot{J}_c is the flux of angular momentum due to convection. For $g = 1$ the convective angular momentum flux is oriented down the angular velocity gradient, while for $g = -1/3$ the convective angular momentum flux is oriented down the specific angular momentum gradient (Narayan et al. 2000). We write the convective diffusion coefficient in a form similar to the definition of viscosity used by Shakura & Sunyaev (1973),

$$\nu_c = \alpha_c \frac{p}{\rho \Omega_K}, \quad (6)$$

where α_c is a dimensionless coefficient that describes the strength of convective diffusion.

Finally, the energy equation is

$$\rho T \frac{ds}{dt} \equiv \frac{1}{\gamma - 1} \left[\frac{\partial p}{\partial t} + v_r \frac{\partial p}{\partial r} \right] + \frac{\gamma}{\gamma - 1} \frac{p}{r^2} \frac{\partial}{\partial r} (r^2 v_r) = Q_{\text{diss}} - Q_{\text{rad}} + Q_{\text{conv}}, \quad (7)$$

in which T is the temperature, s is the specific entropy, γ is the adiabatic index, Q_{diss} is the dissipation rate due to both viscosity and convective shear stress, Q_{rad} is the radiative cooling rate and $Q_{\text{conv}} [= -\nabla \cdot \mathbf{F}_{\text{conv}}]$ is the energy transfer rate due to convection, with $F_{\text{conv}} [= -\nu_c \rho T \partial s / \partial r]$ being the outward energy flux due to convection. The heating rate is expressed by

$$Q_{\text{diss}} = (\nu + g\nu_c) \rho r^2 \left(\frac{\partial \Omega}{\partial r} \right)^2. \quad (8)$$

For the right-hand side of the energy equation, we can write

$$Q_{\text{adv}} = Q_{\text{diss}} - Q_{\text{rad}} + Q_{\text{conv}}, \quad (9)$$

where Q_{adv} is the advective transport of energy. We employ the advection factor, $f = 1 - Q_{\text{rad}}/Q_{\text{diss}}$, that measures how much the flow is advection-dominated (Narayan & Yi 1994). For simplicity we assume the advection factor f to be a constant less than unity.

The mass accretion rate in a quasi-spherical accretion flow can be written as

$$\dot{M}(r, t) = -4\pi r^2 \rho v_r. \quad (10)$$

We will use this quantity in the next section. The mass accretion rate is a constant in the steady state RIAFs, but it varies with position in the present model.

3 SELF-SIMILAR SOLUTIONS

3.1 Analysis

Narayan et al. (2000) studied the above system of equations in the case of a steady state, radially self-similar flow. Here, we seek an unsteady self-similar solution for this system of equations. Thus,

we introduce the self-similar variable ξ and assume each physical quantity is given by the following form:

$$\xi = r(GM_*)^{-1/3}\tau^{-2/3}, \quad (11)$$

$$\rho(r, t) = R(\xi)(\dot{M}_0/GM_*)\tau^{-1}, \quad (12)$$

$$p(r, t) = \Pi(\xi)(\dot{M}_0/(GM_*)^{1/3})\tau^{-5/3}, \quad (13)$$

$$v_r(r, t) = V(\xi)(GM_*)^{1/3}\tau^{-1/3}, \quad (14)$$

$$\Omega(r, t) = W(\xi)\tau^{-1}, \quad (15)$$

$$\dot{M}(r, t) = \dot{M}_0\dot{m}(\xi), \quad (16)$$

where $\tau = (t_0 - t)$, with $t < t_0$, and \dot{M}_0 is a constant whose value can be obtained by typical values of the system. The present model is applied to RIAFs and the accretion rate in these systems is much lower than the accretion rate for the Eddington mass. Thus, we assume for simplicity that $\dot{M}(r, t)$ is only a function of ξ under similarity transformations and ignore its time dependence in the above transformation. Using the similarity solutions, it can be shown that the total angular momentum, $J = 4\pi \int_0^\infty \rho \Omega r^4 dr$, and the disk mass, $M = 4\pi \int_0^\infty \rho r^2 dr$, are proportional to $\tau^{4/3}$ and τ , respectively. Thus our solutions imply that the total angular momentum and the disk mass are decreasing with time. The decrease of total angular momentum and disk mass can be due to a central object that is considered to be arbitrarily small which acts as a sink for mass and angular momentum (Ogilvie 1999). Substitution of the above transformations into the basic Equations (1)–(3) and (7) yields the following dimensionless equations

$$\left(V + \frac{2\xi}{3}\right) \frac{dR}{d\xi} + R = -\frac{R}{\xi^2} \frac{d}{d\xi} (\xi^2 V), \quad (17)$$

$$\left(V + \frac{2\xi}{3}\right) \frac{dV}{d\xi} + \frac{V}{3} = \xi(W^2 - \xi^{-3}) - \frac{1}{R} \frac{d\Pi}{d\xi}, \quad (18)$$

$$R \left[\left(V + \frac{2\xi}{3}\right) \frac{d}{d\xi} (\xi^2 \omega) - \frac{1}{3} (\xi^2 \omega) \right] = \frac{\alpha}{\xi^2} \frac{d}{d\xi} \left[\Pi \xi^{11/2} \frac{dW}{d\xi} \right] + \frac{1}{\xi^2} \frac{d}{d\xi} \left[\alpha_c \Pi \xi^{(8+3g)/2} \frac{d}{d\xi} \left(\Omega \xi^{3(1-g)/2} \right) \right], \quad (19)$$

$$\frac{1}{\gamma - 1} \left[\left(V + \frac{2\xi}{3}\right) \frac{d\Pi}{d\xi} + \frac{5}{3} \Pi \right] + \frac{\gamma}{\gamma - 1} \frac{\Pi}{\xi^2} \frac{d}{d\xi} (\xi^2 V) = f(\alpha + \alpha_c g) \Pi \xi^{7/2} \left(\frac{dW}{d\xi} \right)^2 + \frac{1}{\xi^2} \frac{d}{d\xi} \left[\alpha_c \xi^{7/2} \frac{\Pi}{R} \left(\frac{1}{\gamma - 1} \frac{d\Pi}{d\xi} - \frac{\gamma}{\gamma - 1} \frac{\Pi}{R} \frac{dR}{d\xi} \right) \right]. \quad (20)$$

This system of equations provides a fourth-order system of non-linear ordinary differential equations that must be solved numerically.

3.2 Inner Limit

For a point very near to the center, ξ_{in} , an appropriate asymptotic solution of $\xi = \xi_{\text{in}}$ has the form

$$R(\xi) \sim \xi^{-3/2} (R_0 + R_1 \xi + \dots), \quad (21)$$

$$\Pi(\xi) \sim \xi^{-5/2} (\Pi_0 + \Pi_1 \xi + \dots), \quad (22)$$

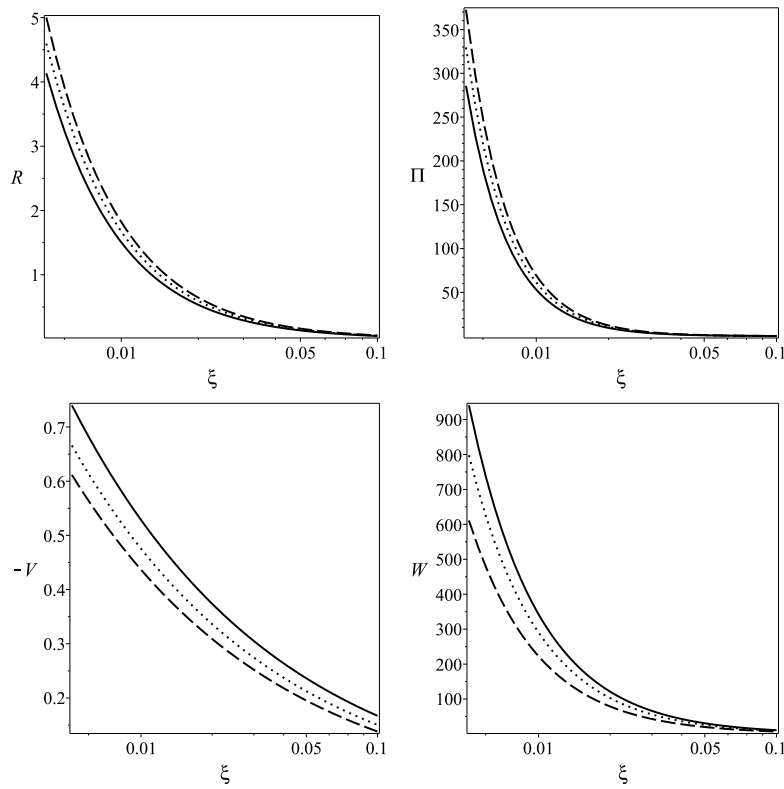


Fig. 1 Time-dependent self-similar solution for $\gamma = 1.5$, $\alpha = 0.1$, $f = 1.0$, $g = -1/3$ and $\dot{m}_{in} = 0.001$. The *solid*, *dotted* and *dashed* lines represent $\alpha_c = 10^{-4}$, 0.04 and 0.07, respectively.

$$V(\xi) \sim \xi^{-1/2}(V_0 + V_1\xi + \dots), \tag{23}$$

$$W(\xi) \sim \xi^{-3/2}(W_0 + W_1\xi + \dots), \tag{24}$$

in which R_0 can be obtained by the following algebraic equation

$$R_0^2 - \frac{\dot{m}_{in}}{12\pi(\alpha + \alpha_c g)} \times \left\{ 5 - \frac{2(\gamma - 5/3)[\alpha + \alpha_c(g - 2/3)]}{f(\gamma - 1)(\alpha + \alpha_c g)} \right\} R_0 - \frac{1}{2} \left(\frac{\dot{m}_{in}}{4\pi} \right)^2 = 0 \tag{25}$$

and the other coefficients are

$$\Pi_0 = \frac{1}{6\pi} \frac{\dot{m}_{in}}{(\alpha + \alpha_c g)}, \tag{26}$$

$$V_0 = -\frac{3}{2}(\alpha + \alpha_c g) \left(\frac{\Pi_0}{R_0} \right), \tag{27}$$

$$W_0^2 = \left(\frac{5/3 - \gamma}{\gamma - 1} \right) \left[\frac{\alpha + \alpha_c(g - 2/3)}{\alpha + \alpha_c g} \right] \left(\frac{\Pi_0}{R_0} \right), \tag{28}$$

where \dot{m}_{in} is the value of \dot{m} at ξ_{in} .

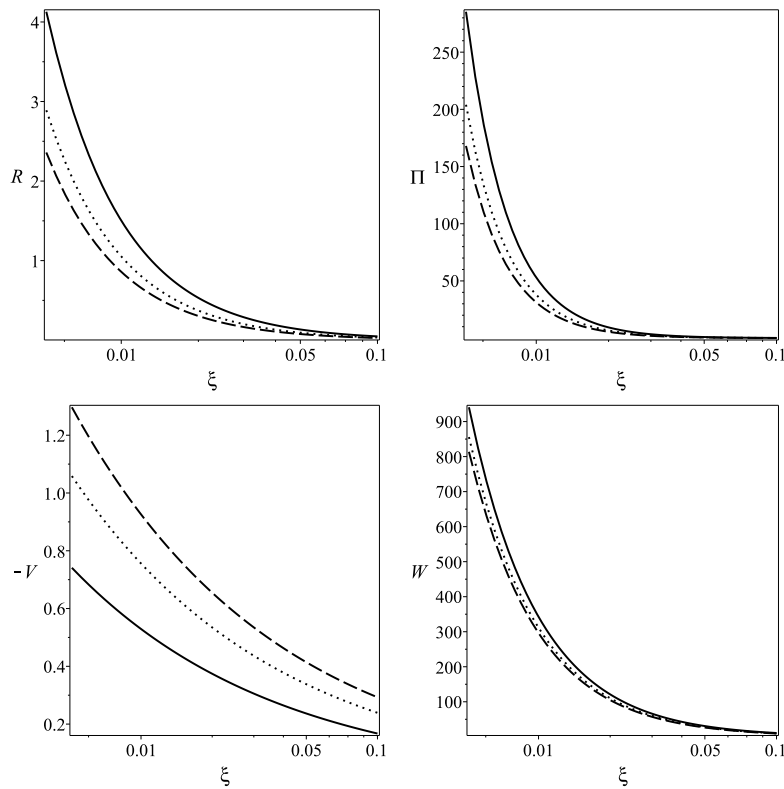


Fig. 2 Same as Fig. 1, but with $g = 1$.

3.3 Numerical Solution

Using a postulated initial value for ξ_{in} , the system of Equations (17)–(20) can be integrated from ξ_{in} outward through the use of expansions \rightarrow (21)–(24). Examples of such solutions are presented in Figures 1–9.

3.3.1 The influences of the convection parameter on physical quantities

Here, we consider the effects of convection on the model in two cases:

- (i) Inward transport of angular momentum, $g < 0$. We choose a negative value for $g [= -1/3]$ to transport the angular momentum inward.
- (ii) Outward transport of angular momentum, $g > 0$. A positive $g [= 1]$ is selected to transport angular momentum outward.

In Figures 1 and 2, the physical quantities have been plotted as functions of the self-similar variable ξ for several values of convection parameter $\alpha_c = 10^{-4}$, 0.04 and 0.07. As can be seen, we have also used a very small value for the convection parameter, $\alpha_c = 10^{-4}$, to compare our model with the accretion flows without convection (e.g. Ogilvie 1999). In Figure 3, we have shown the mass accretion rate as a function of the self-similar variable ξ for several values of $\alpha_c = 0.05$, 0.07 and 0.09.

In the first case, the radial infall velocity with respect to the solution without convection decreases by adding convection parameter α_c , but in the second case, it increases. This happens be-

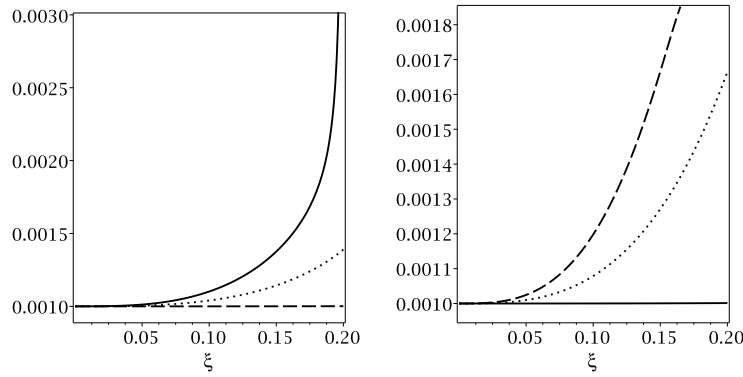


Fig. 3 Time-dependent self-similar solution of mass accretion rate. The input parameters in the left panel are the same as in Fig. 1, but the *solid*, *dotted* and *dashed* lines represent $\alpha_c = 0.05, 0.07$ and 0.09 , respectively. The input parameters in the right panel are the same as in the left panel, but with $g = 1$.

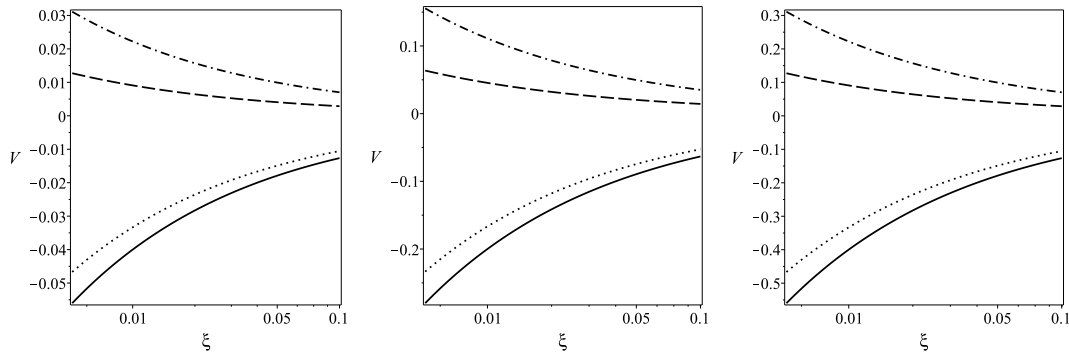


Fig. 4 The radial velocity profiles for several values of the parameters of viscosity and convection. The input parameters for the *left* panel are $\alpha = 0.01$ and the *solid*, *dotted*, *dashed* and *dot-dashed* lines represent $\alpha_c = 0.01, 0.02, 0.04$ and 0.05 respectively. The input parameters for the *middle* panel are $\alpha = 0.05$ and the *solid*, *dotted*, *dashed* and *dot-dashed* lines represent $\alpha_c = 0.05, 0.10, 0.20$ and 0.25 respectively. The input parameters for the *right* panel are $\alpha = 0.1$ and the *solid*, *dotted*, *dashed* and *dot-dashed* lines represent $\alpha_c = 0.1, 0.2, 0.4$ and 0.5 , respectively. In the three panels, we chose $\gamma = 1.5, f = 1.0, g = -1/3$ and $\dot{m}_{in} = 0.001$.

cause, in the first case, the angular momentum is transported inward due to convection, thus, the convection reduces the efficiency of the angular momentum transport outward and the accretion rate. However, in the second case, convection increases the efficiency of the transport of angular momentum outward and the mass accretion rate. These properties can be seen in Figure 3 as the mass accretion rate decreases (or increases) in the first (or second) case by adding α_c . Increases (or decreases) in density with respect to a solution without convection by adding the convection parameter in Figure 1 (or 2) can be due to the behavior of radial infall velocity; in cases of higher (or lower) radial velocity, more (or less) mass will be accreted to the central object and thus the mass density decreases (or increases). In both cases, the angular velocity with respect to the solution without convection decreases by adding the convection parameter α_c . This property is qualitatively in accord with the model presented by Faghei & Omidvand (2012). From Figures 1 and 2, the gas pressure

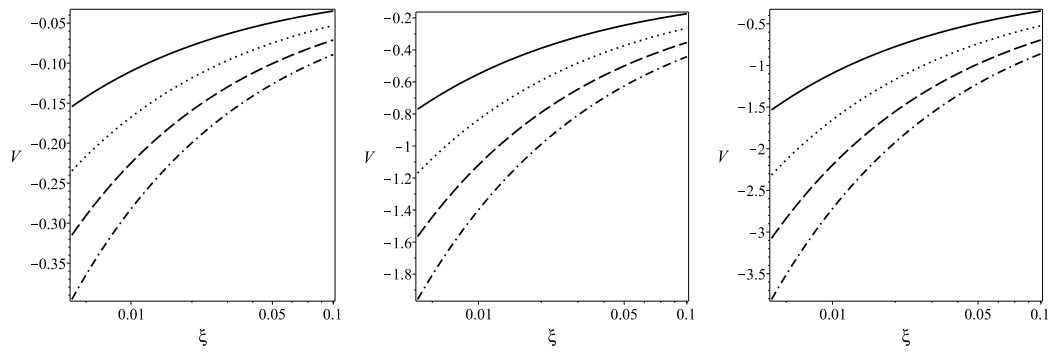


Fig. 5 The radial velocity profiles for several values of the parameters describing viscosity and convection. The input parameters for the *left* panel are $\alpha = 0.01$ and the *solid, dotted, dashed* and *dot-dashed* lines represent $\alpha_c = 0.01, 0.02, 0.03$ and 0.04 , respectively. The input parameters for the *middle* panel are $\alpha = 0.05$ and the *solid, dotted, dashed* and *dot-dashed* lines represent $\alpha_c = 0.05, 0.10, 0.15$ and 0.20 , respectively. The input parameters for the *right* panel are $\alpha = 0.1$ and the *solid, dotted, dashed* and *dot-dashed* lines represent $\alpha_c = 0.1, 0.2, 0.3$ and 0.4 , respectively. In all three panels, we chose $\gamma = 1.5, f = 1.0, g = 1$ and $\dot{m}_{in} = 0.001$.

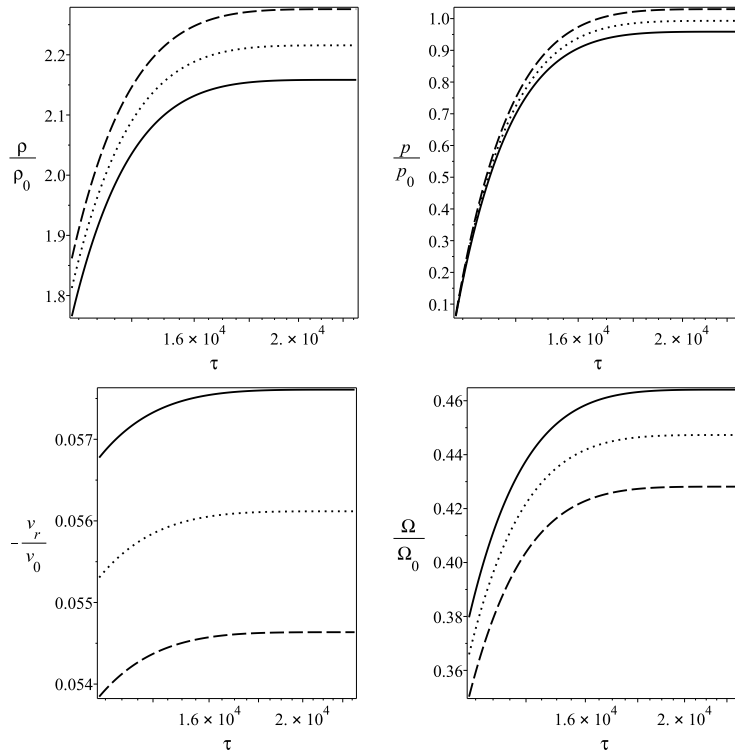


Fig. 6 The variation with time of the physical variables for an arbitrary radius. The input parameters are $\gamma = 1.5, \alpha = 0.1, f = 1.0, g = -1/3$, and $\dot{m}_{in} = 1.0$. The *solid, dotted* and *dashed* lines represent $\alpha_c = 0.01, 0.02$ and 0.03 , respectively. ρ_0, p_0, v_0 and Ω_0 are the constants which make the physical variables non-dimensional.

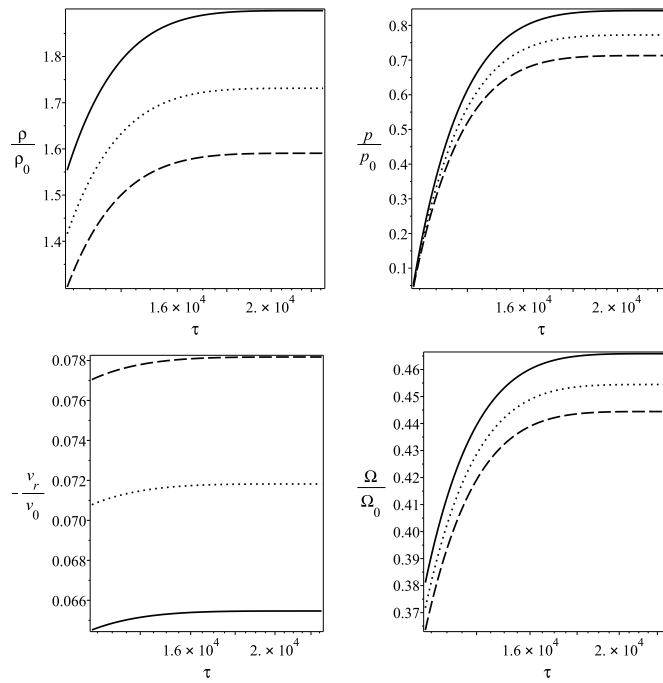


Fig. 7 Same as Fig. 6, but with $g = 1$.

with respect to the solution without convection increases (or decreases) with increasing α_c because the gas pressure is proportional to the density, $p \propto \rho$, thus the gas pressure increases (or decreases) by increasing (or decreasing) density.

In Figures 4 and 5, we consider the effects of the convection parameter on accretion flow with several values for the viscosity parameter. In Figure 4, we use $g = -1/3$, which means angular momentum due to convection is transferred to inner radii. The solutions of Narayan et al. (2000) show that when using a negative value for g and a low value for the viscosity parameter, the accretion velocity may become zero or even change its sign due to convection. This kind of accretion flow is called convection dominated accretion flow (CDAF). In Figure 4, we used three values for viscosity parameter, $\alpha = 0.01, 0.05$ and 0.1 , to consider the effects of CDAFs in the current model. As can be seen in Figure 4, for all values of the viscosity parameter, the effect of CDAF can happen for $\alpha_c \simeq -\alpha/g$, in which $g < 0$. Here, we also consider the radial velocity in the case of angular momentum transfer for several values of the viscosity parameter. As can be seen in Figure 5, the radial velocity is negative for all input parameters of viscosity and convection; thus CDAF does not occur in the case of outward angular momentum transfer, $g > 0$.

In Figures 6 and 7, time evolution of the physical variables has been considered in two cases of inward and outward transport of angular momentum. In both cases, the physical variables decrease with increasing time. We have also considered the influences of the convection parameter on the physical variables. The behavior of physical variables with respect to convection does not change with increasing time. In the case of inward angular momentum transfer, shown in Figure 6, the density and pressure of the gas increased by adding the convection parameter. However, the efficiency of the convection parameter on the density and pressure decreased with increasing time. Although in the case of outward angular momentum transport, the density and pressure of the gas decreased by adding the convection parameter, in this case also, the efficiency of the convection parameter on the density and pressure decreased with increasing time. From Figures 6 and 7, the rotational

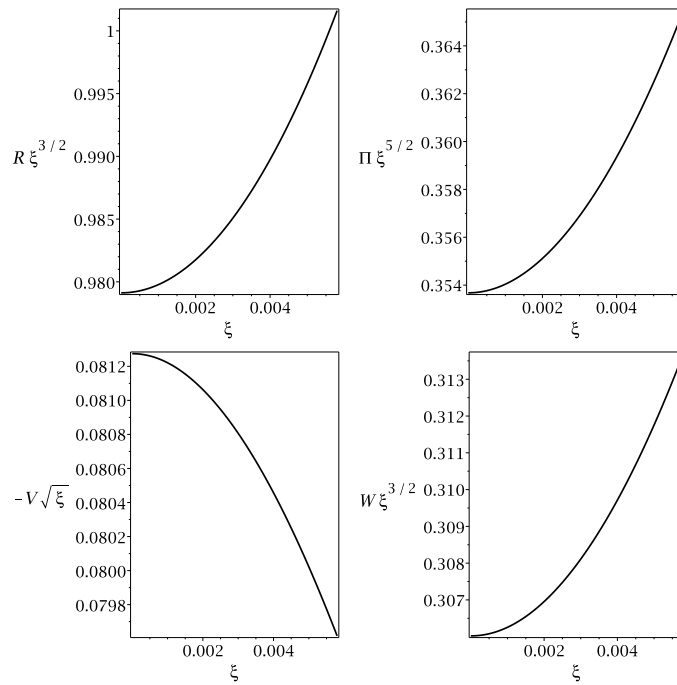


Fig. 8 Comparison of the present model with the steady state self-similar ADAF solutions (e.g. Narayan & Yi 1994). The input parameters are $\alpha = 0.1$, $f = 1.0$, $\alpha_c = 0.05$, $g = 1$, $\dot{m}_{\text{in}} = 1$ and $\gamma = 1.5$.

velocity decreased with the magnitude of convection. However, the effects of convection on the rotational velocity decreased with increasing time. The radial infall velocity for inward (or outward) angular momentum transfer decreases (or increases) by adding the convection parameter. Unlike the other physical variables, the effects of convection on radial infall velocity do not weaken with increasing time.

3.3.2 Comparison of the results with steady state self-similar solutions of ADAFs and RIAFs

In Figures 8 and 9, we compare the unsteady self-similar RIAFs with the steady state, radially self-similar solutions of ADAFs and RIAFs. In the steady state self-similar ADAFs (e.g. Narayan & Yi 1994), $\rho \propto r^{-3/2}$, $p \propto r^{-5/2}$, $v_r \propto r^{-1/2}$, $\Omega \propto r^{-3/2}$ and mass accretion rate is a constant. To compare our results with the steady state self-similar ADAFs, we divide the physical quantities by their radial dependence in the steady state self-similar ADAFs. On one hand, $R/\xi^{-3/2}$, $\Pi/\xi^{-5/2}$, $V/\xi^{-1/2}$ and $W/\xi^{-3/2}$ are constant in the steady state self-similar ADAFs, but as can be seen in Figure 8, they vary with radii in the present model. Like the density, the gas pressure and angular velocity vary more shallowly than their radial dependence in the steady state self-similar ADAFs, and the radial infall velocity varies faster than $r^{-1/2}$.

As mentioned, we have also compared our results with the steady state self-similar RIAFs. In steady state self-similar RIAFs (e.g. Narayan et al. 2000), $\rho \propto r^{-1/2}$, $p \propto r^{-3/2}$, $v_r \propto r^{-3/2}$, $\Omega \propto r^{-3/2}$ and mass accretion rate is a constant. In Figure 9, we divide the physical quantities by their radial dependence in steady state self-similar RIAFs. Profiles of the physical quantities in Figure 9 demonstrate that the density and gas pressure decrease faster than $r^{-1/2}$ and $r^{-3/2}$, respectively, and the radial infall velocity and the angular velocity vary more shallowly than $r^{-3/2}$.

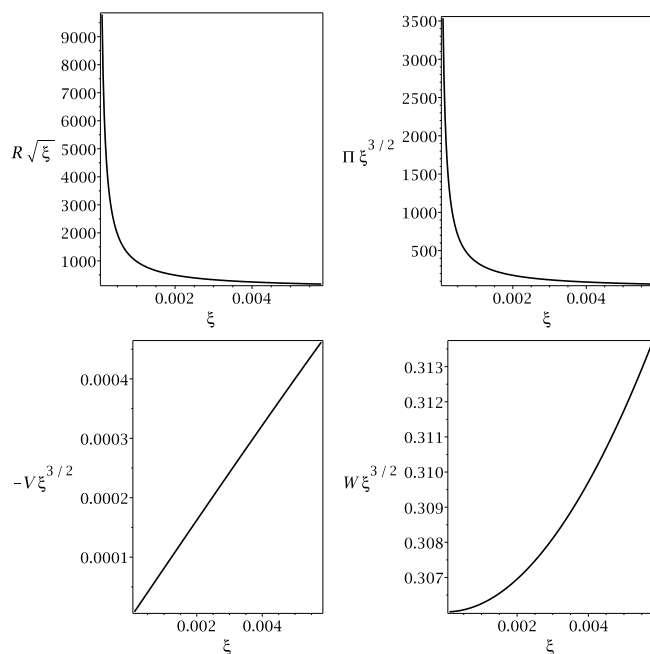


Fig. 9 Comparison of the present model with the steady state self-similar RIAF solutions (e.g. Narayan et al. 2000). The input parameters are the same as in Fig. 8.

From Figures 8 and 9, we conclude that in the unsteady self-similar RIAFs, the radial velocity and the density have a radial dependence between $r^{-1/2}$ and $r^{-3/2}$. On the other hand, the unsteady self-similar RIAFs take an intermediate place between steady state self-similar ADAFs and RIAFs. These properties are in accord with direct numerical simulations of RIAFs (e.g. Igumenshchev et al. 2003) and global studies of RIAFs (e.g. Lu et al. 2004).

4 SUMMARY AND DISCUSSION

In this paper, we investigated the time evolution of radiatively-inefficient accretion flows in the presence of convection. Thus, we adopted models by Ogilvie (1999) and Narayan et al. (2000). Since convection can transport the angular momentum and energy, we applied its effects to the angular momentum and energy equations. We assumed two cases for angular momentum transport due to convection: inward and outward. Since the basic equations were written in a time dependent form, we used the unsteady self-similar method to solve them.

The present model demonstrated the decrease (or increase) in radial infall velocity for inward (or outward) transport of angular momentum due to convection. These properties are qualitatively consistent with previous RIAF models (e.g. Zhang & Dai 2008; Faghei & Omidvand 2012). Moreover, convection simultaneously transports energy outward and angular momentum inward (or outward), strongly suppressing (or supporting) the accretion rate onto the central black hole. These properties are also in accord with previous studies (e.g. Narayan et al. 2000, 2002). In this paper, we compared time dependence of RIAFs with the steady state self-similar RIAFs and ADAFs. The mass accretion rate in the present model varies with radius unlike the steady state solution that is a constant throughout the disk (e.g. Narayan & Yi 1994; Narayan et al. 2000; Lu et al. 2004; Faghei & Omidvand 2012). In this model, the radial infall velocity and the density have a radial dependence between $r^{-1/2}$ and $r^{-3/2}$. These results are consistent with the direct numerical simulation

of RIAFs (e.g. Igumenshchev et al. 2003) and the global study of RIAFs (e.g. Lu et al. 2004). The present dynamical study showed the physical variables decrease with increasing time. The effects of convection on the physical variables, except for the radial infall velocity, decreased with increasing time. In this paper, we assumed the convection to be a free parameter in order to study its effects on the physical quantities, but we could obtain the value of the convective parameter by the use of mixing length theory (e.g. Narayan et al. 2000). The present model can be modified though using mixing length theory in future research.

Acknowledgements I would like to thank the anonymous reviewer for valuable and constructive comments that helped me to improve the initial version of this paper.

References

- Abramowicz, M. A., Chen, X., Kato, S., Lasota, J.-P., & Regev, O. 1995, *ApJ*, 438, L37
 Abramowicz, M. A., Czerny, B., Lasota, J. P., & Szuszkiewicz, E. 1988, *ApJ*, 332, 646
 Balbus, S. A. 2004, *ApJ*, 600, 865
 Di Matteo, T., Allen, S. W., Fabian, A. C., Wilson, A. S., & Young, A. J. 2003, *ApJ*, 582, 133
 Esin, A. A., McClintock, J. E., & Narayan, R. 1997, *ApJ*, 489, 865
 Faghei, K., & Omidvand, M. 2012, *Ap&SS*, 341, 363
 Fukue, J. 2000, *PASJ*, 52, 829
 Fukue, J. 2009, *PASJ*, 61, 1305
 Hawley, J. F., Balbus, S. A., & Stone, J. M. 2001, *ApJ*, 554, L49
 Ho, L. C. 2009, *ApJ*, 699, 626
 Ichimaru, S. 1977, *ApJ*, 214, 840
 Igumenshchev, I. V., Chen, X., & Abramowicz, M. A. 1996, *MNRAS*, 278, 236
 Igumenshchev, I. V., & Abramowicz, M. A. 1999, *MNRAS*, 303, 309
 Igumenshchev, I. V., & Abramowicz, M. A. 2000, *ApJS*, 130, 463
 Igumenshchev, I. V., Abramowicz, M. A., & Narayan, R. 2000, *ApJ*, 537, L27
 Igumenshchev, I. V., Narayan, R., & Abramowicz, M. A. 2003, *ApJ*, 592, 1042
 Igumenshchev, I. V. 2006, *ApJ*, 649, 361
 Kato, S., Fukue, J., & Mineshige, S. 2008, *Black-Hole Accretion Disks* (Kyoto Univ. Press)
 Lu, J.-F., Li, S.-L., & Gu, W.-M. 2004, *MNRAS*, 352, 147
 Machida, M., Matsumoto, R., & Mineshige, S. 2001, *PASJ*, 53, L1
 McKinney, J. C., & Gammie, C. F. 2002, *ApJ*, 573, 728
 Mineshige, S., Kawaguchi, T., Takeuchi, M., & Hayashida, K. 2000, *PASJ*, 52, 499
 Narayan, R., & Yi, I. 1994, *ApJ*, 428, L13
 Narayan, R., McClintock, J. E., & Yi, I. 1996, *ApJ*, 457, 821
 Narayan, R., Igumenshchev, I. V., & Abramowicz, M. A. 2000, *ApJ*, 539, 798
 Narayan, R., Quataert, E., Igumenshchev, I. V., & Abramowicz, M. A. 2002, *ApJ*, 577, 295
 Nemmen, R. S., Storchi-Bergmann, T., Yuan, F., et al. 2006, *ApJ*, 643, 652
 Ogilvie, G. I. 1999, *MNRAS*, 306, L9
 Pen, U.-L., Matzner, C. D., & Wong, S. 2003, *ApJ*, 596, L207
 Popham, R., & Gammie, C. F. 1998, *ApJ*, 504, 419
 Quataert, E., & Gruzinov, A. 2000, *ApJ*, 539, 809
 Shakura, N. I., & Sunyaev, R. A. 1973, *A&A*, 24, 337
 Stone, J. M., Pringle, J. E., & Begelman, M. C. 1999, *MNRAS*, 310, 1002
 Watarai, K.-y., & Mineshige, S. 2003, *ApJ*, 596, 421
 Yuan, F., & Bu, D.-F. 2010, *MNRAS*, 408, 1051
 Yuan, F., Quataert, E., & Narayan, R. 2003, *ApJ*, 598, 301
 Yuan, F., Shen, Z.-Q., & Huang, L. 2006, *ApJ*, 642, L45
 Zhang, D., & Dai, Z. G. 2008, *MNRAS*, 388, 1409